RSC Advances

PAPER

View Article Online
View Journal | View Issue

Cite this: *RSC Adv.*, 2025, **15**, 8729

Porous organic polymers for selective enrichment of trace Cu(II) in food and water samples†

Uzma Haseen, *[a] Sakshi Kapoor,[b] Rais Ahmad Khan [c] and Bon Heun Koo[d]

Received 11th November 2024
Accepted 19th February 2025

DOI: 10.1039/d4ra08024f

rsc.li/rsc-advances

Porous organic polymers (POPs) were synthesized by polymerization of benzene triamine and trimesoyl chloride. The POP material is water-stable and shows selective extraction of Cu(II) due to its intrinsic nitrogen-rich surface, which forms a chelate with Cu(II) ions. The prepared polymeric material was characterized through Fourier transform infrared spectroscopy, X-ray photoelectron spectroscopy, energy-dispersive X-ray elemental mapping, and scanning electron microscopy for surface group analysis and structural morphology studies. A microcolumn was developed using POPs for the preconcentration of trace Cu(II) from complex real samples. The proposed method shows a high enrichment factor of 900 and a quantification limit of 1.1 ppb for Cu(II) ions. The accuracy of the developed method was confirmed by analyzing standard reference materials (NIES 8 and NIES 10c) and the standard addition method. The method shows good precision with an RSD value of less than 5%.

1. Introduction

Copper (Cu(II)) is an essential micronutrient that plays a vital role in human health. [1] It acts as a cofactor for several enzymes involved in energy production, the development of connective tissues, and the protection against oxidative stress. [1,2] Nevertheless, this requirement can have both positive and negative consequences. [3] If the balance of Cu(II) in the body is disturbed and an excessive amount accumulates, it can lead to copper toxicity. [4–6] This toxicity can arise from various sources, such as innate metabolic abnormalities and environmental contamination. Contaminated drinking water is a potential main cause of excessive exposure to Cu(II). Copper pipes in plumbing systems are the primary cause of pollution, particularly when the water is corrosive or the pipe fittings were relatively new and lacks coating for protection. Elevated amounts of copper in the environment, resulting from industrial activity and natural weathering, are deemed dangerous to both aquatic ecosystems and human health.

The precise determination of trace copper levels in water samples is essential for environmental monitoring, assessing water quality, and controlling pollution to protect public health and safeguard drinking water and food sources. [7] Analyzing Cu(II) in low concentrations is often challenging due to the complex composition of natural water. Therefore, it is necessary to employ an analytical preconcentration approach to purify the sample and enhance the detection limits. [8] Considering these facts, the current study was designed to create an extraction method for selectively extracting and quantifying trace quantities of Cu(II) in water samples. The preconcentration procedures established here for enriching the copper content are both sensitive and specific for detecting copper using various analytical methods. Therefore, they provide reliable instruments for protecting water resources and monitoring environmental health. Solid-phase microextraction (SPE) is a method of preparing samples in which the desired substances are separated and concentrated from liquid samples. [9] This method is both cost-effective and widely renowned for its simplicity, speed, and minimal usage of solvents. [10] It is very efficient and can be applied to a wide range of situations. SPE involves the introduction of a tiny quantity of sorbent material into a compact column. The diluted sample solution passes through the column until it reaches a state of equilibrium with the sorbent. At this stage, the analyte adheres to the sorbent and is concentrated by that quantity. Afterward, the analyte that has already been absorbed is removed from the sorbent using an adequate solvent. The eluted analytes are now concentrated and can be directly injected into analytical equipment for further examination. [11] This makes the adaptable technique highly suitable for a wide range of analytical applications.

The utilization of porous organic materials has been advanced to function as a crucial material in the extraction and analysis of minute quantities of heavy metals in water samples. [12–14] Due to their large surface area and unique characteristics, they are capable of efficiently binding and concentrating metal

[a]Department of Chemistry, Aligarh Muslim University, Aligarh 202001, India. E-mail: uzmahaseen.chem@gmail.com
[b]Nanoscale Research Facility, Indian Institute of Technology Delhi, Hauz Khas, New Delhi, 110016, India
[c]Department of Chemistry, College of Science, King Saud University, Riyadh 11451, Saudi Arabia
[d]School of Materials Science and Engineering, Changwon National University, Changwon 51140, Gyeongnam, South Korea

† Electronic supplementary information (ESI) available. See DOI: https://doi.org/10.1039/d4ra08024f

ions, even at low concentrations. [15,16] Nevertheless, despite the notable benefits, there are certain constraints associated with nanomaterials. The synthesis and management of porous nanomaterials might incur significant expenses, particularly when it comes to their practical use in real-world settings. The process is intricate and requires specialized tools and expertise. Moreover, the aggregation of colloidal particles during water analysis poses an additional problem by potentially compromising the sensitivity of the analyte ions. POPs, a new material in SPE, refer to polymeric nanoconstructs that possess sufficient mechanical stability to endure the pressure in their environment. They possess thin, sheet-like structures; typically, these materials are created through the condensation of two or more monomers using condensation polymerization. [17,18] However, they can also form extremely thin sheets, measuring only a few nanometers in thickness, which depends on the concentration of the monomer. [19] Polymeric amphiphilic nanomaterials (POPs) can be utilized in reverse osmosis processes to remove salt from water, as well as in organic solvent nanofiltration. [20,21] Additionally, POPs can be employed to enhance the mechanical stability of materials and create barrier films. [22] Research on polyamide composites, namely those composed of nanosheets, is still in its early stages, but demonstrates significant potential for various applications. Herein, a new polymeric amine containing a polyamide nanosheet (POPs) was created and employed for the first time in the preconcentration and quantification of trace amounts of Cu(II) ions using a solid-phase microextraction technique. The present process utilized a straightforward interfacial polymerization method to react the 1,3,5-benzene-triamine and trimesoyl chloride monomers in their condensation reaction. This results in a rapid and energy-efficient process, without the need for high-energy or specialized equipment and solvents often used in the synthesis of other nanomaterials. Furthermore, this simple reaction would also result in a high degree of purity of the product, as it does not involve the use of a catalyst for production or any secondary substances. The synthesized POPs underwent characterization to analyze their functional groups, surface shape, surface area, and elemental composition before their use in preconcentration investigations.

2. Experimental

2.1. Material and method

All the chemicals used were of analytical reagent grade. 1,3,5-Benzenetriamine, triethylamine, trimesoyl chloride, and *n*-hexane were purchased from Sigma Aldrich. A standard solution of copper nitrate (1000 ppm) was obtained from Agilent. Other metal salts used in this study were obtained from CDH chemicals. Deionized water (DI; 18 MΩ cm; Merck Millipore) was used to prepare a stock of metal ions. Nitric acid (HNO_3), sulfuric acid (H_2SO_4), hydrogen peroxide (H_2O_2) and hydrochloric acid (HCl) were obtained from Merck to elute the metal ions. All the data were measured/repeated three times ($n = 3$), and a mean value with two significant figures has been reported along with the standard deviation.

2.2. Synthesis of POPs

A solution containing 2.0 millimoles per liter of 1,3,5-benzenetriamine monomer was prepared by dissolving it in 40 mL of DI water. To scavenge protons in the aqueous solution, 5.0 mL of triethylamine was added to the amine solution. A stoichiometric amount of trimesoyl chloride co-monomer was dissolved in 10 mL of *n*-hexane, and then slowly added dropwise to a heated amine monomer solution while vigorously stirring for 10 minutes. The polyamide, a white solid, was coagulated and subsequently washed with *n*-hexane, methanol, and an abundant amount of DI water to eliminate any remaining unreacted monomers. The resulting product was subjected to drying at a temperature of 60 °C in a vacuum oven for characterization and further utilization. Fig. 1 illustrates the schematic representation of polyamide synthesis.

2.3. Characterization

The prepared POPs were characterized for functional group analysis by recording the attenuated total reflectance spectra (ATR-IR, Shimadzu), after 64 scans, at a frequency range of 4000–400 cm^{-1}. Scanning electron microscopic (SEM, JSM-7800F, Jeol, Japan) investigations were made to observe the structure and surface morphology. Elemental analysis using energy-dispersive

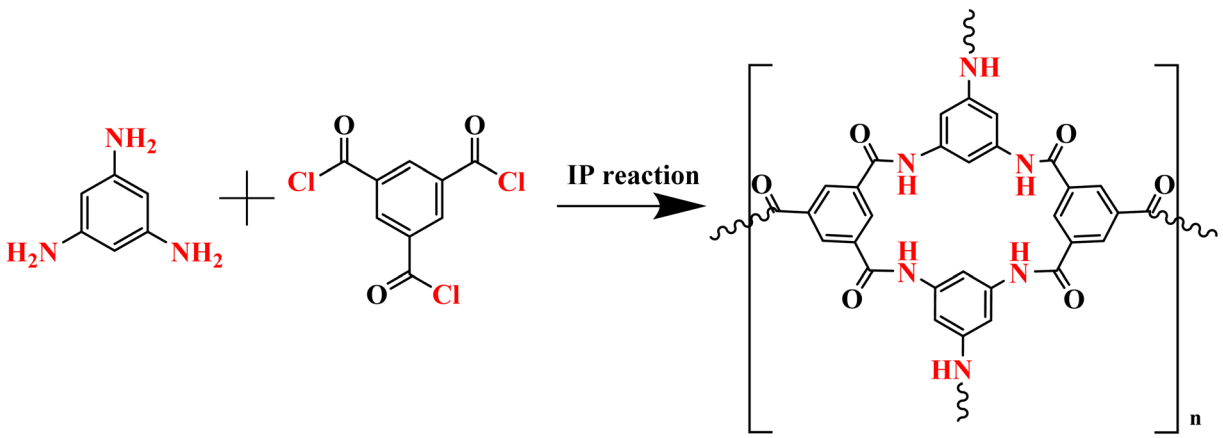

Fig. 1 Schematic diagram illustrating the chemical formation of POPs.

X-ray (EDX, QUANTAX X129 eV, Bruker) data elucidated the percent elemental composition of the obtained polyamide material. The in-depth structural morphology was observed using high-resolution transmission electron microscopy (HRTEM, FEI TECNAI TF20) at an accelerating voltage of 200 kV. A zeta analyzer (zeta potential, Metrohm, US) was used to study the surface charges of POPs. X-ray photoelectron spectroscopic (XPS, model PHI 230 5000, USA) analysis was carried out to evaluate the functional groups and oxidation states. The Brunauer–Emmett–Teller (BET, quanta chrome 232 Nova 2000e) analyzer was used to obtain the specific surface area and pore volume of the POP adsorbent. Inductively coupled plasma optical emission spectrometry (ICP-OES) (Avio 200 PerkinElmer) was used to analyze the concentration of metal ions. To characterize the molecular structure of the prepared POPs, solid state ^{13}C NMR spectra were recorded using a Jeol JNM-ECZL spectrometer (Peabody, MA). The crystallinity of the POPs has been estimated using X-ray diffraction measurements (XRD, Rigaku, India).

2.4. Food sample preparation

Five fish, with a combined weight of 1070.0 ± 0.60 g, were obtained at a local market in Delhi, India. The fish were dissected to extract the flesh. A 10 g sample of the flesh was placed in a Petri plate, and subjected to microwave radiation in a kitchen microwave oven. The sample was then dried (in an air oven) at a temperature of 120 °C until it reached a stable weight. Subsequently, the desiccated samples were moved to digestion flasks, where a mixture of ultrapure concentrated nitric acid and hydrogen peroxide (in a 1 : 1 ratio, volume to volume) was introduced. The digesting flasks were heated to a temperature of 130 °C until all of the ingredients were completely dissolved. The resulting digest was dehydrated by gradually evaporating any remaining liquid and subsequently diluting it with double-distilled water to reach a final amount of 50 mL for further analysis. Furthermore, mushroom specimens were acquired from a local marketplace in Delhi, India. The specimens were cleansed with acetone, dried in an oven, and pulverized using a domestic grinder. The pulverized material was passed through an 80-mesh sieve and kept in a plastic bag until it was analyzed. A 10 g section of the mushroom sample was exposed to 10 mL of concentrated HNO_3, followed by microwave digestion at 800 W for 15 minutes using a ramp program at 120 °C (with no holding time), 160 °C (with a 5 minute holding time), and 180 °C (with a 10 minute holding time), respectively. Following the thorough elimination of HNO_3, the remaining substance was dissolved in a 2 mL solution of 0.5 M HNO_3. It was then transferred to a 50 mL volumetric flask and diluted with deionized water until it reached the designated mark. This was done to facilitate subsequent analysis.

2.5. Recommended column and batch procedure for the preconcentration of Cu(II)

A small glass column containing 200 mg of POP sorbent was filled and balanced with a 100 mL solution of Cu(II) at the required concentration. The solution was passed through the column at a flow rate of 5 mL min^{-1} using a peristaltic pump. To investigate the impact of pH on the adsorption of Cu(II), the pH of the solution was methodically modified from pH 2 to 7 by introducing tiny quantities of 0.1 M HNO_3 and 0.1 M NaOH. Following the passage of the sample solution through the column, the packed column was flushed with deionized water to eliminate any metal ions that were not absorbed. Afterward, the Cu(II) ions that were attached to the POPs were removed by using a suitable stripping agent at a flow rate of 2 mL min^{-1}. This reduced flow rate permitted efficient mass transfer between the solid POPs and the liquid phase, ensuring comprehensive elution of the adsorbed Cu(II). The eluent, which contained the desorbed Cu(II) ions, was subsequently examined using inductively coupled plasma optical emission spectrometry (ICP-OES) to determine the precise quantity of Cu(II) that was first adsorbed onto the POPs.

For studying the effect of the sample pH, the sample pH of the simulated solutions (100 mL; 500 μg mL^{-1}) was adjusted within the range of pH 2 to 7 by utilizing an appropriate amount of HNO_3 and/or NaOH solutions. The effect of the adsorbent amount was studied to ascertain the most suitable quantity of POPs needed for efficient preconcentration of trace Cu(II) ions. Several quantities of the substance, ranging from 50 to 250 mg, were filled into a set of columns. Subsequently, a solution with a volume of 100 mL and a concentration of 10.0 μg mL^{-1} of Cu(II) ions was passed through each column at a sample pH of 6.0. Similarly, the effect of the sample flow rate of the column on the process of sorption and elution was optimized using a 100 mL solution containing 5 μg of Cu(II), which was buffered at a pH of 6 ± 0.1, and passed through the column at flow rates varying from 2 to 10 mL min^{-1}. The sorbed metal ions were eluted and analyzed later.

3. Result and discussion

3.1. Characterization

3.1.1 Chemical analysis. The ATR-IR spectra of the amine monomer, nascent POPs and after complexation with Cu(II) (POP–Cu) (Fig. 2) reveal several prominent bands indicative of its molecular structure. A broad absorption band centered at

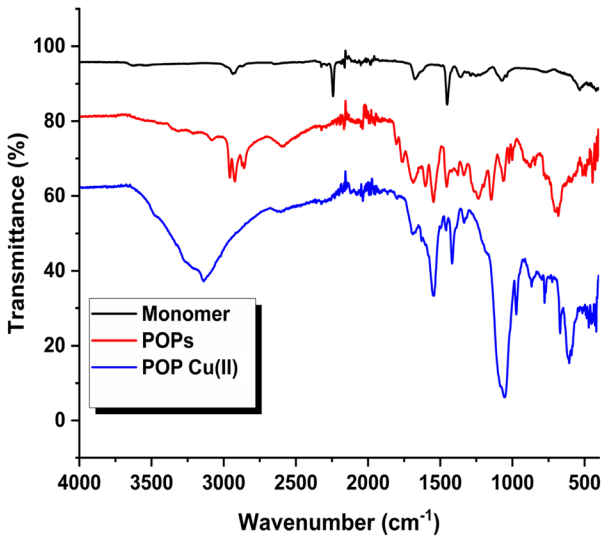

Fig. 2 FTIR-ATR spectra of the amine monomer, POPs and POP–Cu(II) complex.

3000 cm^{-1} corresponds to the stretching vibrations of N–H bonds, encompassing contributions from the –NH functional groups. [23] Specific peaks that were observed include the C=O stretching vibrations at 1690 cm^{-1}, C–N stretching vibrations at 1065 cm^{-1}, O=C–N stretching vibrations at 1620 cm^{-1} and additional C–O stretches at 1225 cm^{-1} and 1105 cm^{-1}.[23] Vibrations associated with C–C bonds are evident at 1445 cm^{-1} and 1487 cm^{-1}. The spectrum also displays N–H bending at 1604 cm^{-1}, with N–H wagging vibrations appearing at 754 cm^{-1} and 695 cm^{-1}. Furthermore, the O–H deformation is noted at 1366 cm^{-1}. Distinct peaks at 3025 cm^{-1} and 2920.8 cm^{-1} correspond to sp^3 C–H and sp^2 C–H stretching vibrations, respectively. These spectral features collectively characterize the chemical composition and structural elements of POPs, providing insights into their molecular properties that are essential for understanding their applications in metal ligand complexation.

The solid state ^{13}C NMR spectrum of the prepared POPs shows the characteristic chemical shifts corresponding to different carbon environments in the polymer backbone (Fig. S2†). The characteristic peak for the amide carbonyl (C=O) carbon appears at 174.8 ppm. Similarly, the aromatic carbon peaks in the benzene rings resonate between 120–150 ppm, with carbons (attached to nitrogen and carbonyl groups) appearing at around 148 ppm. Carbons directly bonded to nitrogen in the aromatic system typically resonate at 144 ppm. These distinct signals provide structural confirmation of the structural order, aiding in the analysis of the POP composition and functionality. The X-ray diffraction (XRD) analysis of synthesized POPs shows a semi-crystalline structure (Fig. S3†). The spectra typically exhibit broad diffraction peaks, indicating a combination of ordered and disordered regions within the polymer matrix. The presence of sharp reflections at specific 2θ values (typically around 32°) corresponds to the crystalline domains possibly formed by π–π interactions between the aromatic rings, while the broad halo-like background suggests the existence of amorphous regions. The observed semi-crystalline nature enhances the polymer's mechanical strength, making it suitable for column operation.

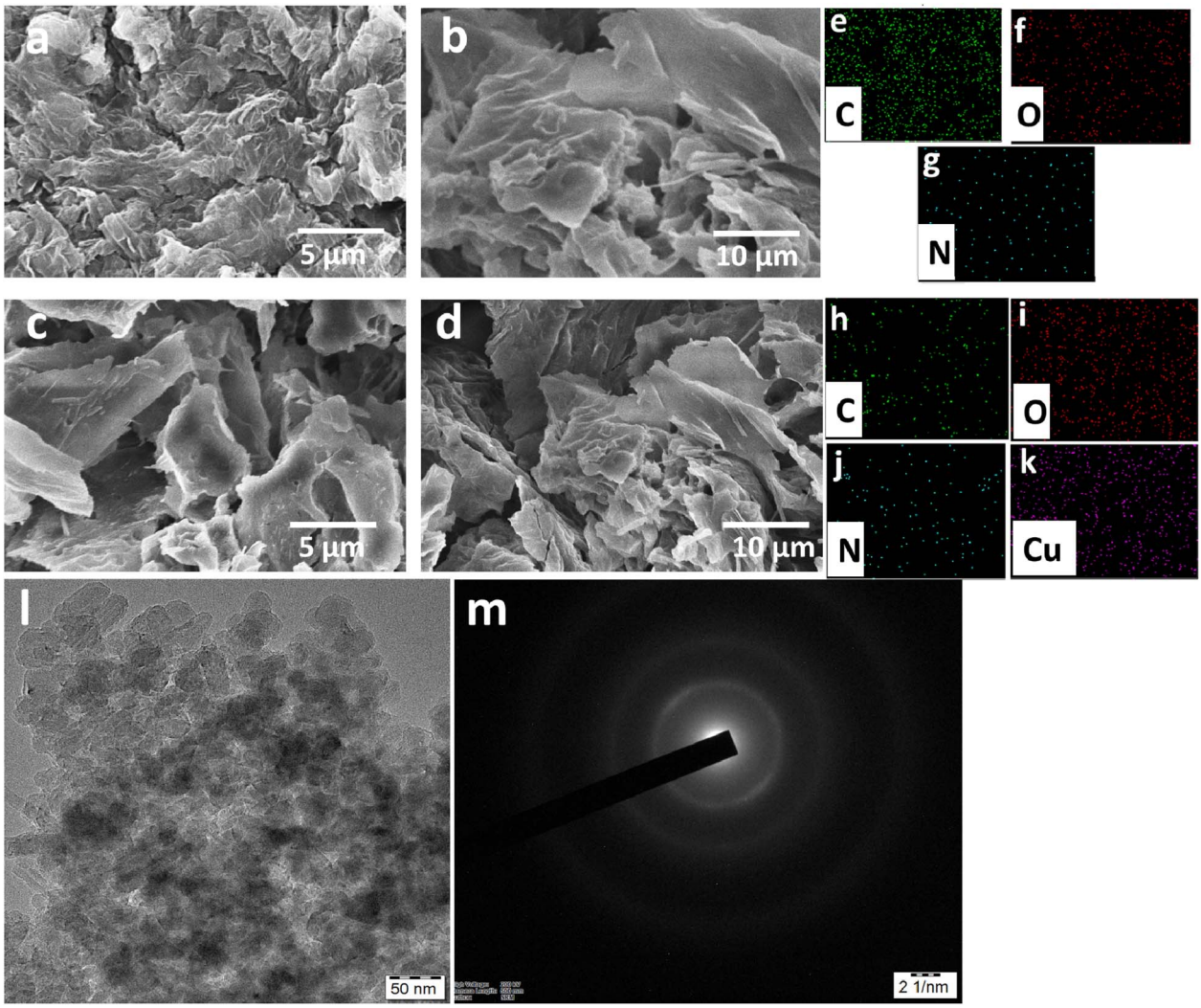

Fig. 3 SEM micrographs of POPs (a and b) and POP–Cu(II) sorbent (c and d) at different magnifications and their respective elemental analysis (e–k); TEM micrograph of POPs (l) and the corresponding SAED pattern, illustrating the amorphous morphology of POPs (m).

(a) Topography. Fig. 3a–d demonstrates that the scanning electron microscopy (SEM) pictures of POPs and POP–Cu(II) complex exhibit a surface morphology characterized by homogeneous and wrinkled sheets-like structure. The presence of a smooth surface morphology is essential for accurate analysis and material durability, as it suggests a minimal occurrence of surface defects such as fractures or cavities. The polyamide nanosheets were analyzed using EDS of SEM micrographs (Fig. 3e–k) to determine their elemental components, which consist of carbon, oxygen, nitrogen, and copper. The results indicate that the surface components are uniformly distributed within the POP adsorbent. This suggests that the successful bonding of both 1,3,5-benzenetriamine and trimesoyl chloride leads to the formation of a POP adsorbent. HRTEM was employed to investigate the morphology and structural characteristics of the synthesized porous organic polymers (POPs). Fig. 3l reveals a well-defined porous architecture, confirming the presence of an interconnected network with uniform pore distribution. The observed porosity is consistent with the results obtained from BET analysis, indicating a high surface area and sufficient pore volume for efficient adsorption applications. In Fig. 3m, the observed SAED pattern is attributed to the amorphous nature of the prepared POP material. This nanoscale framework and structural integrity of the POPs demonstrate their suitability for metal ion extraction and other separation processes. In addition, XPS analysis was carried out to ascertain the presence and oxidation state of the surface components, thereby verifying the existence of the surface functionality on the POP adsorbent. Table 1 presents the comprehensive elemental data obtained from the XPS analysis of the POP adsorbent.

(b) Porosity. A nitrogen gas adsorption–desorption investigation was conducted to assess the physical properties of the adsorbent. The average surface area, pore radius, and pore volume of the polyamide adsorbent were determined using the Brunauer–Emmett–Teller (BET) method. The values obtained were 718.15 $m^2 g^{-1}$, 68.52 nm, and 2.18 $cm^3 g^{-1}$, respectively. The study focused on determining the point of zero charge (pHz) of the POP adsorbent in order to analyze its surface charge (Fig. 4a). It was observed that the surface carries a negative charge at a pH of 4.0. Furthermore, the charge density increased as the pH of the sample increased, reaching a value of −23 eV at a pH of 7.0. This amplifies the electrostatic contact between the adsorbent and the metal ions, hence improving the adsorption efficacy.

3.2. Effect of sample pH

The ability of a polymeric adsorbent to bind metal ions effectively over a wide range of pH values is essential and depends on the rivalry between metal ions and protons in water-based solutions for the same binding sites on the adsorbents. Fig. 4b demonstrates that the absorption of Cu(II) by the POP adsorbent commences under acidic conditions (pH 2 ± 0.1), and has less retention of Cu(II) compared to conditions of pH 3 and higher. Based on the concepts of hard and soft acid–base theory, the POP adsorbent, which has a soft 'N-donor atom with a lone pair of electrons' in the molecular structure, can form a complex with the soft acid Cu(II) containing vacant d-orbitals, allowing it to selectively bind to this metal ion. [24,25] The process of protonation at low solution pH, which leads to the formation of a positive charge, has a negligible impact on the basicity of the nitrogen atom. As the pH rises above 2, the level of protonation falls, reducing the competition between metal and hydrogen ions while simultaneously increasing the nitrogen basicity. As a result, the adsorbent ability to adsorb Cu(II) is improved, and this improvement is consistent across a wide range of pH levels. Moreover, from Fig. 4a, it was observed that before the pH value of 3.7, the surface carries a positive charge. This was not favorable for the interaction of the positively charged cations at the surface of the materials, thus causing a reduction in the adsorption efficiency. However, at pH values above 4.0, the surface has a negative charge density. This charge density increases as the pH of the sample increases, reaching a value of −23 eV at a pH of 7.0. It amplifies the electrostatic contact between the adsorbent and the metal ions, hence improving the adsorption efficacy. Nevertheless, within the pH range of 6 to 7, the absorption of Cu(II) exhibits a similar sorption, potentially attributed to the negative surface charge of POPs at both pH values. The highest level of Cu(II) absorption capacity, which is necessary for the effective preconcentration of small amounts of analytes, is attained when the pH value is between 6 and 7. The POPs exhibits preferential affinity for Cu(II) ions compared to other metals under optimum conditions. The selective adsorption of Cu(II) by the nitrogen-containing POPs is supported by the electron-rich and spatial arrangement of nitrogen-containing functional groups. The nitrogen-rich POPs effectively bind and differentiate copper from other ions. The electron-rich nitrogen centers enhance copper binding through stronger σ-donation, which is in line with hard–soft acid–base principles where Cu(II) forms favorable interactions with nitrogen donors. Herein, the complex stability is often enhanced *via* conjugation with the π-electron of the adjacent substituent ring (Fig. 1). This chelation effect not only stabilizes the metal ion, but also reduces the competition from other metal ions. Moreover, the POPs with uniformly distributed nitrogen sites create an environment that favors the formation of stable Cu(II) chelates. This molecular fitting can

Table 1 Elemental data of POP sorbent obtained through XPS analysis

Element	Peak position (eV)	Height cps	Fwhm (eV)	Area (*p*) cps eV	Atomic%
C 1s	285.58	26 713.77	1.90	28 314.36	62.51
O 1s	531.94	33 598.79	1.42	75 754.54	22.34
N 1s	402.43	1597.11	1.36	3867.28	15.15

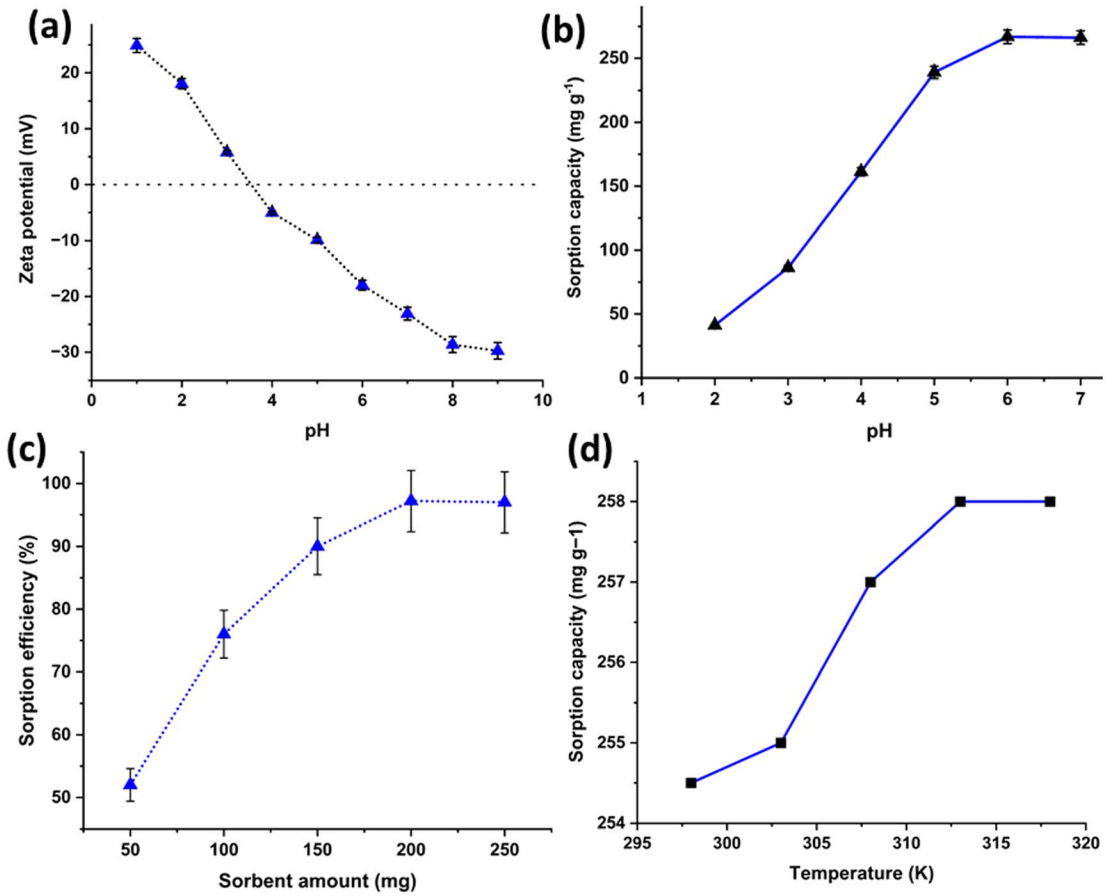

Fig. 4 (a) Zeta potential of the measurement of POPs; (b) effect of the solution pH on Cu(II) adsorption, (sample volume, 100 mL; concentration, 500 μg mL^{-1}; sorbent amount, 200 mg; flow rate, 5 mL min^{-1}); (c) effect of the sorbent amount on Cu(II) adsorption, (sample volume, 100 mL; concentration, 10 μg mL^{-1}; sample, pH 6; flow rate, 5 mL min^{-1}); (d) effect of temperature on the adsorption of metal ions.

lead to high selectivity even in the presence of competing metal ions. Remarkably, POPs demonstrate considerable specificity for Cu(II) at pH 6.0 (Fig. 4), resulting in an improved sorption capacity of 254.5 mg g^{-1}. Therefore, a pH value of 6.0 ± 0.1 was chosen as the most suitable pH for the following studies.

3.3. Effect of the adsorbent amount and sample temperature

The studies showed that the ability to retain Cu(II) ions increases in proportion to the quantity of the polymer, reaching a maximum of 200 mg g^{-1} of material (Fig. 4c). No additional increase in retention was detected beyond this quantity, suggesting that full absorption occurred at a dosage of 200 mg. The insufficient active sites for the analyte ion interaction at the lower adsorbent amount results in the low adsorption of Cu(II). Thus, after optimization, it was determined that 200 mg of POPs was the most effective quantity and was subsequently employed for further investigations.

The effect of temperature on the Cu(II) adsorption has been studied by equilibrating the 200 mg of POPs with 50 mL of sample containing 500 mg per L Cu(II) ions (pH 6) in the temperature range of 298–318 K. The POPs were equilibrated with the sample solution for 3 h, using a mechanical shaker with a temperature controller. It was observed that upon increasing the temperature, the adsorption of metal ions slightly increases from 255 to 257 mg g^{-1} at the elevated temperature of 308 K and reached a maximum of 258 mg g^{-1} at 313 K. Above this temperature, no significant increase in the adsorption was determined. The obtained results are shown in Fig. 4d.

3.4. Eluting agent and column reusability test

We performed a set of experiments to remove the trapped Cu(II) from POPs using several mineral acids, namely nitric acid (HNO_3) and hydrochloric acid (HCl). By varying the volumes and concentrations of acids now called eluents (as shown in Fig. 5a and b), we optimized the recovery of Cu(II) ions. Achieving a quantitative recovery of Cu(II) (>99%) was made possible by utilizing 3.0 mL of a 1.5 M HNO_3 solution. Therefore, a volume of 3.0 mL of a 1.5 M solution of HNO_3 was chosen as the eluting agent for further investigations. The effect of other eluents, concentrations, and varying volumes on the recovery of Cu(II) are mentioned in Fig. 5b. To evaluate the potential for reusing POPs, the material was subjected to several cycles of sorption and elution. A solution with a volume of 100 mL and containing 5 μg of Cu(II) was run through the column at a flow rate of 5 mL min^{-1}. The solution was buffered to a pH of 6.0 ± 0.2. To remove the Cu(II) that was held back, a solution of 3.0 mL of 1.5 M HNO_3 was

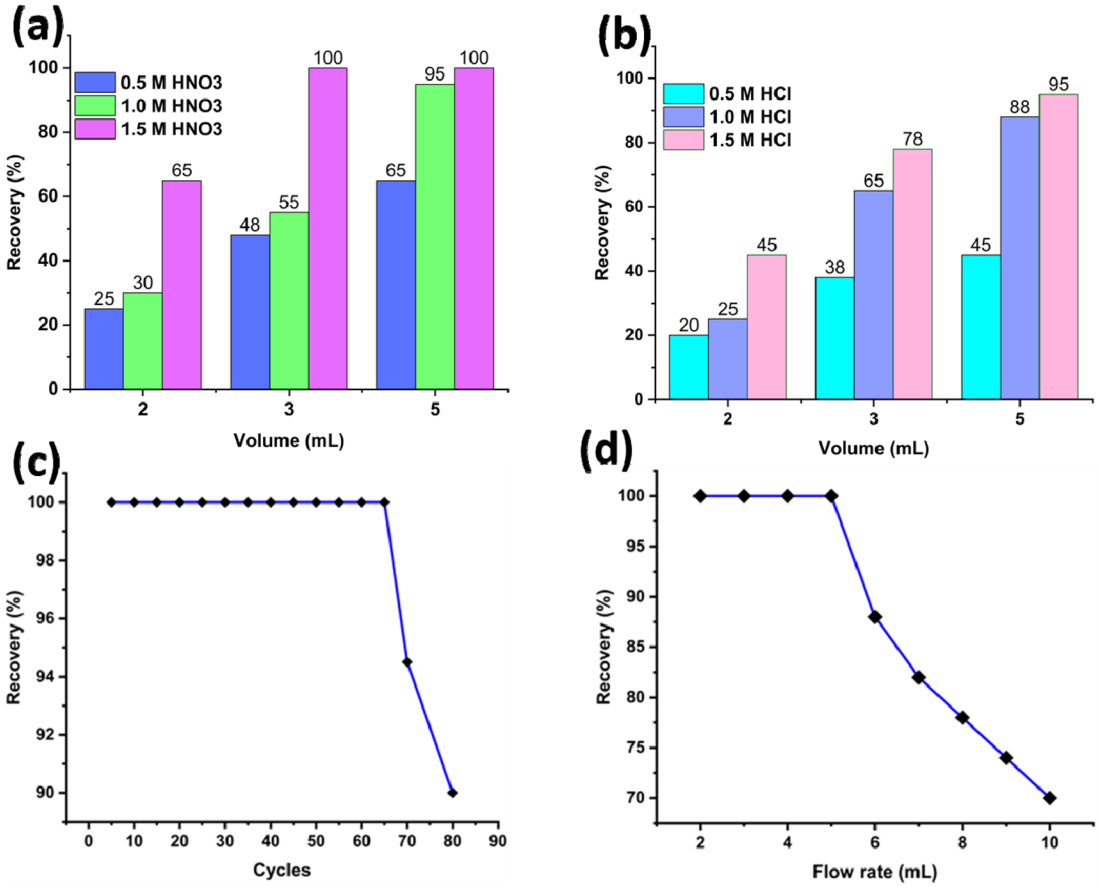

Fig. 5 (a and b) Effect of various eluting agents on the recovery of the sorbed amount of Cu(II), (sample volume, 100 mL; concentration, 50 μg mL^{-1}; sample, pH 5; eluent flow, 2 mL min^{-1}); (c) reusability of the POP sorbent for multiple adsorption–desorption cycles; (d) effect of the flow rate on the sorption of metal ions.

passed through at a rate of 2 mL min^{-1}. The column bed was effectively repurposed for a maximum of 65 cycles without experiencing any reduction in its sorption capacity (Fig. 5c). Afterward, there was a noticeable decline of 5.5% in the recovery of sorbed analyte until the 70th cycle. This decrease is likely attributed to the degradation of functional groups of the solid matrix. The consistent Cu(II) uptake capacity observed in both the first and 65 cycles indicates that POPs can be reused without significant loss in capacity. This suggests that there is minimal functionality loss during the sorption/elution cycles. Thus, POPs can be efficiently utilized iteratively for the specific isolation and enrichment of Cu(II) from polluted water sources.

In addition, the chemical stability of POPs has been studied by equilibrating the material (200 mg) with 50 mL of 2 M HCl and NaOH solution individually for 24 h. Afterward, the adsorption of metal ions was checked and compared with the untreated material. No significant changes in the adsorption of metal ions was observed, thus showing the material chemical stability in both acidic and basic media.

3.5. Optimal flow rate for the sorption/desorption of Cu(II)

The results demonstrated that the column was able to sustain quantitative retention of Cu(II) up to a flow rate of 5 mL min^{-1}, indicating rapid kinetics. The retention decreased at flow rates over 5 mL min^{-1}, with a fall of 12.0% observed at 6 mL min^{-1} (Fig. 5d). This decline can be attributed to the shortened time required for the phases to reach equilibrium. Consequently, a sorption flow rate of 5 mL min^{-1} was chosen for further trials. The residence time at the ideal flow rate of 5 mL min^{-1} was determined to be 9.6 seconds (0.16 minutes) for a column filled with 0.2 g of POPs in a column with dimensions of 10 cm × 1.0 cm in diameter. The impact of the elution flow rate was investigated in elution investigations by utilizing 3.0 mL of 1.5 M HNO_3. The best elution flow rate was determined to be 2 mL min^{-1}, resulting in the removal of almost 99% of the residual Cu(II).

3.6. Preconcentration studies

To examine the levels of trace metals and study how the volume of a sample affects the recovery of Cu(II), we conducted an experiment where sample volumes varying from 500 to 3000 mL, each containing a consistent quantity of 3 μg Cu(II), were passed through a column. Following the column operation, the Cu(II) that was retained was separated using 3.0 mL of eluent and quantified by ICP-OES. The findings demonstrate that it is possible to achieve a quantitative recovery (>99%) of Cu(II) for sample volumes up to 2700 mL, and elute the sorbed amount in

3 mL of eluent. This corresponds to a preconcentration limit of 1.1 μg L^{-1} and a significant preconcentration factor of 900. Furthermore, the concentration of 1.1 μg L^{-1} cannot be fully retrieved from a 100 mL sample volume because of the small amount of analyte (0.11 μg in 100 mL), which would not produce a linear calibration curve.

3.7. Interference studies

We investigated the impact of the simultaneous presence of other ionic species on the preconcentration of Cu(II). To gather the data, a series of solutions with a sample size of 50 mL, containing 5 μg of Cu(II) and varying concentrations of interferents, were preconcentrated using the developed column procedure. The obtained results are shown in Table 2, which establish the tolerance level against co-ions as the highest concentration of accompanying substances that produce an absorbance error of no more than ±5% in comparison to the absorbance of the eluent for a 100.0 μg L^{-1} solution of Cu(II) alone, following solid-phase extraction (SPE). The results indicate that none of the ions present at the investigated concentrations had any negative impact on the specific preconcentration and measurement of Cu(II). Therefore, POPs demonstrate two notable characteristics: it differentiates copper from both inorganic and organic interferences by means of selective chelation, and it concurrently concentrates small quantities of copper in the sample solution.

Table 2 Cu(II) ion extraction from the binary mixture of co-existing ions (experimental conditions: pH 6; total volume, 50 mL; flow rate, 5 ml min^{-1}; metal ion concentration, 10 μg L^{-1})

	Tolerance ratio [added ions/metal ion] (μg L^{-1})
Added ions	Cu(II)
Na^+ ($NaCl$)	3.25×10^4
K^+ (KCl)	4.25×10^4
NH_4^+ (NH_4Cl)	5.25×10^4
Ca^{2+} ($CaCl_2$)	5.25×10^5
Mg^{2+} ($MgCl_2$)	5.18×10^4
CH_3COO^- (CH_3COONa)	6.00×10^4
Cl^- ($NaCl$)	6.50×10^6
Br^- ($NaBr$)	6.50×10^6
SO_4^{2-} (Na_2SO_4)	5.60×10^5
CO_3^{2-} (Na_2CO_3)	5.54×10^5
PO_4^{2-} (Na_2PO_4)	3.58×10^4
NO_3^{2-} (Na_2NO_3)	5.55×10^5
Humic acid	88.0
Fulvic acid	72.0

3.8. Analytical method validation

The accuracy of the method was evaluated by analyzing Standard Reference Materials (SRMs), and by recovering the spiked analytes from real samples. The Student's *t*-test values for mean Cu(II) concentrations in SRMs (NIES 8: 1.19 and NIES 10C: 4.1) were found to be below the critical value of 4.303 at a 95% confidence level for a sample size of $N = 3$ (Table 3). This indicates that there is no significant bias in the presence of other elements. The recovery studies consisted of adding predetermined quantities of Cu(II) to real samples at two different concentrations, as documented in Table 4. The average percentage recoveries varied between 98.5% and 106%, with a relative standard deviation (RSD) below 5%. This indicates that the approach is reliable for the accurate determination of Cu(II) in different matrices, without any substantial interference. The approach demonstrated excellent precision, as evidenced by a coefficient of variation below 3.25% for five repeated measurements of 1 μg of copper in a 100 mL solution. A calibration curve for Cu(II) was established by concentrating standards (ranging from 0 to 50 μg L^{-1}) using optimal conditions and including a blank run without any metal ions. The correlation coefficient (R^2) for the calibration fit was found to be 0.9998, and the regression equation is $A = 17.9853X_{Cu} + 2.1206$. The limit of detection (LOD) and limit of quantification (LOQ) were determined using a calculation based on the standard deviation of the mean blank absorbance signal and the slope of the calibration curve. [26] The LOD was found to be 0.02 μg L^{-1}, while the LOQ was determined to be 0.066 μg L^{-1}. This was established by following 20 consecutive runs of the blank sample, where a procedural control experiment was conducted using the prescribed column protocol with 100 mL of an aqueous solution containing an appropriate buffer (without metal ions). The elution was carried out with a 3 mL volume before performing ICP-OES determination. The signals were recorded and the mean average value was calculated. The obtained LOD and LOQ are comparable and better than the other previous reports for the enrichment and determination of trace metal ions in food and water samples. [1,2] The analytical features of merits of the proposed material have been compared and are summarized in Table 5.

3.9. Application of the method

To assess the suitability of the suggested solid phase extraction (SPE) method for real-world applications, the concentration of

Table 3 Analyses of Cu(II) content in standard reference materials (column parameters: sample volume, 100 mL; sample flow rate, 5 mL min^{-1}; eluent volume, 3 mL; eluent flow rate, 2 ml min^{-1})

Samples	Certified values (μg g^{-1})	Values obtained using the proposed method (μg g^{-1}) ± standard deviation[a]	Values of *t*-test[b]
NIES 8	1.19	1.12 ± 0.04	2.13
NIES 10C	4.1	4.05 ± 0.13	1.85

[a] Mean value ± standard deviation, $N = 3$. [b] At 95% confidence level.

Table 4 Preconcentration and determination of Cu(II) ions in real samples (column parameters: pH 6.0; sample flow rate, 5 mL min^{-1}; sample volume, 1 L; eluent volume, 3 mL; eluent flow rate, 2 mL min^{-1})

		Metal ion found (μg L^{-1}) ± standard deviation[a] (% recovery)
Samples	Amount added (μg)	Cu(II)
Fish[b]	0	0.45 ± 0.03
	3	3.43 ± 0.07 (99.9)
	5	5.48 ± 0.05 (106.6)
Mushroom[b]	0	1.58 ± 0.05
	3	4.47 ± 0.15 (100)
	5	6.58 ± 0.14 (100)
Electroplating waste water	0	12.84 ± 1.05
	3	15.83 ± 1.13 (99.9)
	5	17.85 ± 1.10 (100.1)
River water	0	7.22 ± 0.04
	3	10.20 ± 0.22 (99.0)
	5	12.20 ± 0.12 (99.7)
Ground water	0	nd[c]
	3	2.99 ± 0.08 (99.9)
	5	5.10 ± 0.14 (102)

[a] $n = 3$. [b] μg g^{-1}. [c] Not detected.

Table 5 Comparison of the analytical features of merits of the proposed method with other recent reports

Materials	Sorption capacity (mg g^{-1})	Preconcentration factor	LOQ (ppb)	Technique	Ref.
POPs	254.5	900	1.1	ICP-OES	This work
Fe_3O_4@HOF	146.5	—	1.3	XRF	27
$CoSn(OH)_6$ nanocubes	—	102	0.9	FAAS	28
Al_2O_3@Se@Cys	—	85	4.5	—	29
Fe_3O_4@APTES	—	21	0.9	ICP-OES	30
$MnFe_2O_4$@CBH/CTS	—	—	1.8	G-FAAS	31

Cu(II) was specifically measured in different real water and food samples. This measurement was carried out using the optimized column approach, and the results were reported with a 95% confidence limit. The amount of Cu(II) determined in real samples was found to be 12.84 μg L^{-1} in pretreated electroplating wastewater and 7.22 μg L^{-1} in river water samples, as shown in Table 4. In fish and mushroom samples, the average amount of Cu(II) for three replicate measurements was found to be 0.45 μg g^{-1} and 1.58 μg g^{-1}, respectively. The validity of the method was assessed by systematically altering the sample size ($n = 3$), which eliminates any potential sources of consistent errors, and showcases its effectiveness in the accurate determination of the concentration of Cu(II) ions.

4. Conclusion

An effective approach was established by selecting the monomers and preparing the polyamide porous organic polymer through an environmentally friendly single-step synthesis procedure. The obtained tetradentate chelating structure exhibits a stable complex with Cu(II), and improves the selectivity towards Cu(II) in the presence of other interferent ions in the systems. The POP sorbents exhibit mechanical robustness, as indicated by their multiple use, and a high selectivity for Cu(II) throughout a broad range of solution pH values. The suggested column approach is user-friendly, precise, and replicable with the ability to preconcentrate trace Cu(II) from concentrations as low as 1.1 μg L^{-1}. The cost-effective SPE method enables precise determination without any influence from common co-ions. The reported method has effectively been used to analyze the amount of Cu(II) in tap water, river water, and electroplating wastewater samples. Its reliability has been confirmed by its accurate and precise performance in real samples and certified reference materials. Despite its promising results, the synthesized POPs have some limitations. Under extreme acidic conditions, the column did not show long-term stability, and potential degradation of the Cu(II) adsorption has been observed. Additionally, while the selectivity for Cu(II) is high, interference from structurally similar metal ions at elevated concentrations has been observed. Future studies might focus on expanding the scope of this method to other heavy metal ions, specifically for Pb(II) and Cd(II) from batter waste. In addition, integrating this material into automated or portable detection systems can lead to real-time or onsite monitoring of trace elements.

Data availability

The data obtained and/or used in this study have been provided in the manuscript.

Conflicts of interest

There are no conflicts to declare.

Acknowledgements

The authors extend their gratitude to the Research Supporting Project (RSP2025R400), King Saud University, Riyadh, Saudi Arabia.

References

1 J. C. Dabrowiak, Metal Ion Imbalance in the Body, *Metals in Medicine*, 2019, p. 329.
2 A. T. Jan, M. Azam, K. Siddiqui, A. Ali, I. Choi and Q. M. R. Haq, Heavy Metals and Human Health: Mechanistic Insight into Toxicity and Counter Defense System of Antioxidants, *Int. J. Mol. Sci.*, 2015, **16**(12), 29592.
3 R. G. Lucchini, M. Aschner, D. C. Bellinger and S. W. Caito, Chapter 15 – Neurotoxicology of Metals, in *Handbook on the Toxicology of Metals*, ed. G. F. Nordberg, B. A. Fowler and M. Nordberg, Academic Press, San Diego, 4th edn, 2015, p. 299.
4 G. Crisponi and V. M. Nurchi, Metal Ion Toxicity, *Encyclopedia of Inorganic Chemistry*, 2015.
5 X. Sun, M. Wuest, Z. Kovacs, A. D. Sherry, R. Motekaitis, Z. Wang, *et al.*, In vivo behavior of copper-64-labeled methanephosphonate tetraaza macrocyclic ligands, *J. Biol. Inorg. Chem.*, 2003, **8**(1–2), 217.
6 P. B. Tchounwou, C. G. Yedjou, A. K. Patlolla and D. J. Sutton, Heavy metal toxicity and the environment, *Exper. Suppl.*, 2012, **101**, 133–164.
7 M. Jaishankar, T. Tseten, N. Anbalagan, B. B. Mathew and K. N. Beeregowda, Toxicity, mechanism and health effects of some heavy metals, *Interdiscip. Toxicol.*, 2014, **7**(2), 60.
8 Z. Xu, Q. Zhang, X. Li and X. Huang, A critical review on chemical analysis of heavy metal complexes in water/wastewater and the mechanism of treatment methods, *Chem. Eng. J.*, 2022, **429**, 131688.
9 C. Zhang, H. Xing, L. Yang, P. Fei and H. Liu, Development trend and prospect of solid phase extraction technology, *Chin. J. Chem. Eng.*, 2022, **42**, 245.
10 M. Ferdous Alam, Z. A. Begum, Y. Furusho, H. Hasegawa and I. M. M. Rahman, Selective separation of radionuclides from environmental matrices using proprietary solid-phase extraction systems: A review, *Microchem. J.*, 2022, 107637.
11 U. Haseen and H. Ahmad, Preconcentration and Determination of Trace Hg(II) Using a Cellulose Nanofiber Mat Functionalized with MoS2 Nanosheets, *Ind. Eng. Chem. Res.*, 2020, **59**(7), 3198.
12 H. Ahmad, R. Ahmad Khan, B. Heun Koo and A. Alsalme, Cellulose Nanofibers@ZrO2 membrane for the separation of Hg(II) from aqueous media, *J. Phys. Chem. Solids*, 2022, **168**, 110812.
13 H. Ahmad and C. Liu, Ultra-thin graphene oxide membrane deposited on highly porous anodized aluminum oxide surface for heavy metal ions preconcentration, *J. Hazard. Mater.*, 2021, **415**, 125661.
14 H. Ahmad, C. Cai and C. Liu, Separation and preconcentration of Pb(II) and Cd(II) from aqueous samples using hyperbranched polyethyleneimine-functionalized graphene oxide-immobilized polystyrene spherical adsorbents, *Microchem. J.*, 2019, **145**, 833–842.
15 H. Ahmad, F. M. Husain and R. A. Khan, Graphene oxide lamellar membrane with enlarged inter-layer spacing for fast preconcentration and determination of trace metal ions, *RSC Adv.*, 2021, **11**(20), 11889.
16 H. Ahmad, I. I. B. Sharfan, R. A. Khan and A. Alsalme, Effective Enrichment and Quantitative Determination of Trace Hg2+ Ions Using CdS-Decorated Cellulose Nanofibrils, *Nanomaterials*, 2020, **10**(11), 1–12.
17 J. A. Lee, J. Y. Kim, J. H. Ahn, Y.-J. Ahn and S. Y. Lee, Current advancements in the bio-based production of polyamides, *Trends Chem.*, 2023, **5**(12), 873–891.
18 Y. Feng, X. Li, T. Ma, Y. Li, D. Ji, H. Qin, *et al.*, Preparation of chemically recyclable bio-based semi-aromatic polyamides using continuous flow technology under mild conditions, *Green Chem.*, 2024, **26**(9), 5556–5563.
19 M. Long, L. Yang, T. Wu, M. Zhang, S. Zhang, D. An, *et al.*, A sub-10 nm polyamide nanofiltration membrane from polyvinylpyrrolidone-mediated interfacial polymerization, *J. Membr. Sci.*, 2024, **700**, 122729.
20 F. Panagiotou, I. Zuburtikudis, H. Abu Khalifeh, E. Nashef and V. Deimede, GO and surfactant assisted regulation of polyamide nanofiltration membranes for improved separation performance, *Sep. Purif. Technol.*, 2025, **352**, 128220.
21 J.-B. Li, C.-Y. Zhu, H.-N. Li, J.-H. Xin, H.-Y. Fan, C. Zhang, *et al.*, Polyamide thin-film composite membranes with enhanced interfacial stability for durable organic solvent nanofiltration, *J. Membr. Sci.*, 2024, **704**, 122841.
22 M. Hriberšek, S. Kulovec, A. Ikram, M. Kern, L. Kastelic and F. Pušavec, Technological optimization and fatigue evaluation of carbon reinforced polyamide 3D printed gears, *Heliyon*, 2024, **10**(13), e34037.
23 G. Socrate, Infrared and Raman Characteristic Group Frequencies: Tables and Charts. 3rd ed (The University of West London, Middlesex, U.K.). J. Wiley and Sons: Chichester. 2001. 348 ISBN: 0-471-85298-8, *J. Am. Chem. Soc.*, 2002, 1830.
24 P. K. Chattaraj, H. Lee and R. G. Parr, HSAB principle, *J. Am. Chem. Soc.*, 1991, **113**(5), 1855.
25 R. G. Pearson, The HSAB principle—more quantitative aspects, *Inorg. Chim. Acta*, 1995, **240**(1–2), 93–98.
26 G. L. Long and J. D. Winefordner, Limit of Detection A Closer Look at the IUPAC Definition, *Anal. Chem.*, 1983, **55**(07), 712A.
27 L. Chen, G. Lan, Y. Xu, X. Li and X. Mao, Functionalized magnetic hydrogen-bonded organic framework for

preconcentration and rapid detection of lead and copper ions in water, *Microchem. J.*, 2025, **209**, 112599.

28 A. Bahçıvan, M. Şaylan, O. Sagdic and S. Bakırdere, CoSn(OH)6 nanocubes as a solid sorbent for the effective preconcentration of copper ions in cinnamon (Cinnamomum zeylanicum) extract, *Food Chem.*, 2024, **447**, 139037.

29 T. Golgoli, K. Ghanemi and F. Buazar, Cysteine-functionalized selenium nanoparticles for efficient extraction and preconcentration of cadmium, copper, lead, and zinc ions from environmental water samples, *J. Mol. Liq.*, 2024, **393**, 123680.

30 C. Caner, M. Y. Ciftci, S. Tabassum, H. Altundag and E. Bulut, Novel Triton X-114 coated Fe3O4 magnetic nanoparticle adsorbent for Cd(II) and Co(II) ions preconcentration in honey samples using magnetic solid-phase extraction: Determination by ICP-OES, *J. Mol. Struct.*, 2025, **1321**, 139836.

31 S. M. M. Attaf, R. Alotaibi, A. A. Alotaibi and S. M. Abdel Azeem, Magnetic solid-phase extraction of trace elements in water and fish using greenly synthesized MnFe2O4 @ cabbage hydrochar/chitosan ternary composite, *J. Food Compos. Anal.*, 2025, **137**, 106883.